Clim Dyn (2008) 30:687–701
DOI 10.1007/s00382-007-0316-z

Sensitivity of simulated wintertime Arctic atmosphere to vertical resolution in the ARPEGE/IFS model

Øyvind Byrkjedal · Igor Esau · Nils Gunnar Kvamstø

Received: 27 June 2006 / Accepted: 6 September 2007 / Published online: 16 October 2007

Abstract The current state-of-the-art general circulation models, including several of those used by the IPCC, show considerable biases in the simulated present day high-latitude climate compared to observations and reanalysis data. These biases are most pronounced during the winter season. We here employ ideal vertical profiles of temperature and wind from turbulence-resolving simulations to perform a priori studies of the first-order eddy-viscosity closure scheme employed in the ARPEGE/IFS model. This reveals that the coarse vertical resolution (31 layers) of the model cannot be expected to realistically resolve the Arctic stable boundary layer. The curvature of the Arctic inversion and thus also the vertical turbulent-exchange processes cannot be reproduced by the coarse vertical mesh employed. To investigate how turbulent vertical exchange processes in the Arctic boundary layer are represented by the model parameterization, a simulation with high vertical resolution (90 layers in total) in the lower troposphere is performed. Results from the model simulations are validated against data from the ERA-40 reanalysis. The dependence of the surface air temperature on surface winds, surface energy fluxes, free atmosphere stability and boundary layer height is investigated. The coarse-resolution run reveals considerable biases in these parameters, and in their physical relations to surface air temperature. In the simulation with fine vertical resolution, these biases are clearly reduced. The physical relation between governing parameters for the vertical turbulent-exchange processes improves in comparison with ERA-40 data.

Keywords GCM · Large eddy simulation · Parameterization · Arctic · Stable boundary layer · ARPEGE

Ø. Byrkjedal · I. Esau · N. G. Kvamstø
Bjerknes Centre for Climate Research,
University of Bergen, Allegaten 55,
5007 Bergen, Norway

Ø. Byrkjedal · N. G. Kvamstø
Geophysical Institute, University of Bergen,
Allegaten 70, 5007 Bergen, Norway

I. Esau
Nansen Environmental and Remote Sensing Center,
Thormoehlensgate 47, 5006 Bergen, Norway

Ø. Byrkjedal (✉)
Kjeller Vindteknikk, PO-Box 122, 2027 Kjeller, Norway
e-mail: oyvind.byrkjedal@vindteknikk.no

1 Introduction

The vertical resolution of climate models has not been the focus of many sensitivity studies. This is remarkable because the non-linear vertical profiles of all model variables usually exhibit strong curvature in the first 1 km above the surface. The lower part of the atmosphere comprises the densest clouds and most intense turbulent activity. Sufficient resolution within this layer is thus important both for climate and weather prediction simulations. The models contributing to the IPCC Fourth Assessment Report (AR4) employ vertical resolutions in the range of 12–56 vertical levels for the total atmosphere column (IPCC climate model documentation, http://www-pcmdi.llnl.gov/ipcc/model_documentation/ipcc_model_documentation.php). The majority have only 4–8 layers below the 850 hPa level of the atmosphere.

Earlier studies were able to compare only very coarse resolution models. Improving the vertical resolution from a few kilometers spacing to a few hundred meters was found to not significantly affect the simulation results (Boville

1991). However, Tompkins and Emanuel (2000) demonstrated that equilibrium climate simulations were not possible for models with coarse vertical resolution in the planetary boundary layer (PBL). For vertical resolution coarser than 25 hPa (about 200 m) within the PBL, they found that the temperature and moisture profiles did not converge toward radiative–convective equilibrium. Sensitivity studies on this issue are quite limited, but they generally report beneficial effects of improving the vertical resolution of general circulation models (GCMs) (e.g., Hogan and Brody 1993; Lane et al. 2000; Slingo et al. 2004; Roeckner et al. 2006; Ruti et al. 2006). Bossuet et al. (1998) studied differences in the ARPEGE climate for simulations with 41 and 31 vertical levels (41L and 31L respectively), but did not find any significant changes in the polar troposphere. However, their 41L run retained quite coarse resolution in the boundary layer with the 3 first levels at 43, 140 and 281 m. Recent studies of sensitivity to changes the vertical resolution (e.g. Lane et al. 2000) suggest that considerable refinement (60 vertical levels or more) is needed to achieve visible improvement in the simulations.

The Arctic inversion is the typical situation for the lower atmosphere at high latitudes during winter. The temperature is quite low at ground level and increases to a maximum at 500–1,500 m height. A negative radiation balance at the surface combined with strong air subsidence in the mid-troposphere and the temperature inversion inhibits the development of turbulent mixing in the Arctic. The weak turbulent mixing is unable to compensate the radiative cooling of the surface by increasing the downward heat flux from the warm atmospheric inversion layer (Overland and Guest 1991). The persistent surface cooling results in a gradual formation of very low wintertime temperatures in the lower troposphere. The heat fluxes in the Arctic winter atmosphere are generally directed downward toward the surface. The factors that determine the magnitude of the heat fluxes are the static stability, given by the lapse rate, and wind speed. Stronger winds are related to stronger wind-shears and more turbulent conditions in the PBL. This allows air from higher up in the inversion to be mixed down to the surface. Stronger winds in the Arctic are thus associated with larger downward fluxes of heat and higher surface temperatures. These features of the Arctic wintertime temperature profiles were generally not resolved by the earlier sensitivity studies of vertical resolution.

Inadequacies in describing the turbulent fluxes in the lower troposphere also affect the simulated surface air temperatures (SAT). Walsh et al. (2002) reported generally warm biases over the Arctic Ocean in the models contributing to the IPCC TAR compared to NCEP reanalysis data (Kalnay et al. 1996), while the models contributing to the IPCC AR4 showed generally cold biases over the Arctic Ocean in comparison with ERA-40 reanalysis data (Chapman and Walsh 2007). This development could be related to changes in the model specifications regarding flux adjustments or to changes in the treatment of sea ice in the models. Walsh et al. (2002) also presented the SAT biases for the models from the atmospheric model intercomparison project (AMIP II). These models generally have a warm bias in the Arctic winter.

The summary report on Arctic climate and modelling (ACIA 2004) revealed a serious discrepancy between observed and modelled geographical patterns of the Arctic climate evolution over the last 50 years. The models tend not to produce low temperatures in response to weak wind, but raise the temperature rather rapidly in response to warm air advection. This tends to cause a positive SAT bias, with the largest warm bias located in areas with the climatologically lowest surface temperatures (Kiehl and Gent 2004 for CCSM-2). Cuxart et al. (2006) found in general an overestimation of the fluxes in the turbulence parameterization schemes implemented in research and operational models. Such schemes use constraints on the minimum possible flux (Louis 1979; Beljaars and Viterbo 1999) in order to prevent atmosphere–surface decoupling and consequent model instabilities.

The excessive turbulent fluxes found by Cuxart et al. (2006) lead one to question the reliability and performance of the stable boundary-layer (SBL) parameterizations, greatly affect the Arctic climate. A popular, but undesirable, solution is to tune the schemes towards ideal data sets (e.g. for the ARPEGE model, see Bazile et al. 2005). To our knowledge, however, those tuning exercises have been limited to particular in situ cases and thus suffer from a lack of generality. At present, mainstream studies try to improve model performance in cold climates through development of even more sophisticated vertical diffusivity schemes. The intercomparison by Cuxart et al. (2006) showed that the more sophisticated schemes do not necessarily show a better performance compared to simpler schemes. But one cannot expect to gain full benefit of the advances in the boundary-layer parameterizations if the PBL and lower troposphere remain constrained by a relatively coarse vertical resolution (Bushell and Martin 1999 for 19L).

Dethloff et al. (2001) compared the performance of single-column GCM models (ECHAM3 and HIRLAM) employing analytical turbulence diffusion schemes of the resistance-law type (Zilitinkevich and Esau 2005) with more traditional, eddy-viscosity type schemes employed in the same models. The analytical schemes demonstrated a considerable improvement. The main assumption in the first order closure—(FOC) eddy viscosity scheme is that the vertical turbulent fluxes of heat and momentum can be

expressed in terms of the vertical gradients in model-resolved temperature and momentum. Our hypothesis is that this assumption is violated by the choice of vertical resolution commonly applied for the lower troposphere. By increasing the vertical resolution in this part of the atmosphere our aim is to show a general improvement in the performance of the FOC scheme applied in the model. Our focus will be on the Arctic stable boundary layer, and specifically on heat fluxes and temperature profiles. Overestimation of vertical mixing and turbulent heat fluxes in the stably stratified Arctic atmosphere, which is a common problem for the schemes applied in GCMs (Cuxart et al. 2006), will lead to an excessive heating of the surface. One objective is to show that the reduced vertical mixing obtained by increasing the vertical resolution in the lower troposphere also reduces the atmospheric influx of heat to the surface and thus also the simulated surface temperatures in the Arctic.

Here we investigate the effect of vertical resolution refinement on the model climate. Using guidelines from turbulence-resolving models (e.g. Beare et al. 2006), we determine an adequate spacing for the model vertical levels. We compare simulations with 31 (31L) and 90 (90L) vertical levels. Section 2 describes the ARPEGE GCM and the formulation of the vertical-diffusivity scheme in the model along with the model setup. In Sect. 3, we perform a priori analysis on coarse versus fine vertical mesh. The a priori study incorporates data from a turbulence-resolving model. Climatologies from ERA-40 and the two GCM simulations are presented in Sect. 4. In Sect. 5 we study changes in the basic physical relationships induced by the resolution refinement. Section 6 contains a discussion, and conclusions are given in Sect. 7.

2 Model description

2.1 Turbulence vertical diffusion scheme

Although refinement of the vertical resolution will affect almost all parameterizations in the model, especially the cloud and radiation schemes, here we focus primarily on the turbulence diffusion scheme. In the dry, wintertime Arctic atmosphere, this scheme is an important component in forming the temperature profile in the lowest 500 m (Dethloff et al. 2001). The ARPEGE/IFS model is the atmospheric component of the Bergen climate model (Furevik et al. 2003). It was developed by Meteo-France and ECMWF (Deque et al. 1994). ARPEGE/IFS is a spectral model and the horizontal resolution is here given by a triangular truncation at wavenumber 63 (T63) with linear reduced Gaussian grid equivalent to quadratic T42 (2.8°) for the surface fields. The vertical resolution is described as a hybrid sigma coordinate (Simmons and Burridge 1981). It follows the topography in the lower atmosphere, but becomes gradually parallel to the pressure surfaces at higher levels. The vertical diffusion scheme was developed by Geleyn (1988). It is a first-order eddy-viscosity scheme, which is popular in global models because of its simplicity and physical clarity.

Let ψ be one of the prognostic variables (horizontal components of the wind velocity, moisture or dry static energy). The evolution of ψ due to turbulent transport is given by

$$\frac{\partial \psi}{\partial t} = \frac{1}{\rho}\frac{\partial}{\partial z}\left(\rho K_\psi \frac{\partial \psi}{\partial z}\right) = -g\frac{\partial F_\psi}{\partial p}, \tag{1}$$

where ρ is the air density and g is the acceleration due to gravity. A change in the vertical flux with pressure can be regarded as either convergence or divergence of ψ at a given level and thus gives an increase or decrease in the value ψ by time. The exchange coefficients are either heat, K_h, or momentum, K_m, diffusivities. The exchange coefficient for moisture is assumed to be equal to K_h. They depend on the prognostic variables according to

$$K_m = l_m^2\left|\frac{\partial \vec{U}}{\partial z}\right| \cdot f_m(\mathrm{Ri}) \quad \text{and} \quad K_h = \frac{l_m l_h}{l_m^2}\frac{f_h(\mathrm{Ri})}{f_m(\mathrm{Ri})}K_m \tag{2}$$

where $f_\psi(\mathrm{Ri})$ is a stability function (Louis 1979) and Ri is the gradient Richardson number. The mixing length scale $l_\psi(z)$ characterizes changes in the turbulent eddy size as a function of the distance from the surface. An empirical polynomial fit is adopted

$$l_\psi(z) = az^3 + bz^2 + \kappa z,$$
$$\begin{cases} a = \dfrac{\kappa H - 2\lambda_\psi}{H^3} \\ b = \dfrac{3\lambda_\psi - 2\kappa H}{H^2} \end{cases} \tag{3}$$

where H is the boundary layer depth, λ_ψ is the asymptotic length scale at $z = H$, and $\kappa = 0.4$ is the von Karman constant. The asymptotic length scales for heat (λ_h) and momentum (λ_m) obey the following relation: $\lambda_h = \lambda_m\sqrt{15/2}$. λ_m are prescribed by the model: λ_m=20 m.

Following Troen and Mahrt (1986), the PBL depth, H, is defined as the level where the bulk Richardson number, based on the difference between quantities at a specific level and the lowest surface, reaches the critical value of 0.5. The formulation reads:

$$Ri_j = \frac{(\theta_{vj} - \theta_{v0})gz_j}{\theta_{v0}|\vec{U}_j|^2} \tag{4}$$

here θ_{vj} is the virtual potential temperature at level j, and θ_{v0} is the virtual potential temperature at the surface, $|\vec{U}_j|$ is the wind speed and z_j is the distance of level j from the surface.

The stability functions are given by

$$f_m^{-1} = 1 + 2b\mathrm{Ri}(1 + d\mathrm{Ri})^{-0.5}, \text{and}$$
$$f_h^{-1} = 1 + 3b\mathrm{Ri}(1 + d\mathrm{Ri})^{+0.5} \quad (5)$$

where $b = d = 5$. It produces a realistic Prandtl–Richardson relation, $\mathrm{Pr}(\mathrm{Ri}) = l_m f_m / l_h f_h \gg 1$ for large Ri.

2.2 Experimental design

To study the effect of vertical resolution, two simulations have been set up according to AMIP2 requirements and recommendations (AMIP Newsletter, Gleckler 1996). The model is run with prescribed sea-surface temperatures (SSTs) for the period January 1979–December 1997 (Smith and Reynolds 2004).

The first run, 31L, follows the standard setup of ARPEGE/IFS. The model was set up with 31 vertical layers, where 8 layers were below 1,600 m. The lowest level was at approximately 40 m height and the next level close to 140 m. To assure model consistency with differentiation, the PBL height, H, in the 31L configuration was not allowed to be lower than to 200 m, equivalent to 2.5 model levels. The time step used for this model integration was 1,800 s.

To investigate the effect of increased model resolution within the PBL, we performed a run with a vertical mesh of 90 levels, hereafter denoted 90L. The resolution was improved only for the lower troposphere below 3,000 m. The lowest 5 model levels were located at 10, 20, 30, 40 and 50 m. Above 50 m the vertical resolution decreased. In total, 30 layers were added to the lowest 1,000 m and 30 layers were added between 1,000 m and 3,000 m. The minimum H was reduced to 20 m, equivalent to 2 model levels. The time step was reduced to 900 s to avoid numerical instability. In all other aspects, the diffusion scheme for the two simulations was identical. To check the sensitivity of the model regarding constraints on H, we also performed a 90L simulation with H constrained to a minimum value of 200 m. Regarding the vertical profiles, the results of both 90L runs were very similar. Such a fine vertical resolution in the 90L run should be adequate with regard to most problems related to the coarse mesh representation of strongly curved flux profiles. Only the results from the model run with minimum H constrained to 20 m will be reported in this paper.

To discern the effects of the vertical resolution on the simulated climate, we focus our attention to the PBL height, H, and the vertical temperature gradient. H depends on the bulk Richardson number and gives a good estimate of the depth or intensity of the vertical mixing in the boundary layer. Changes in the vertical exchange processes are manifested by modifying the vertical temperature profile.

3 Scheme properties on coarse versus fine vertical meshes: a priori test

Observations reveal that the Arctic wintertime PBL is typically very shallow (Mahrt and Vickers 2006). The mean depth is commonly less than 150 m. This implies that in standard resolution models only 1–4 levels are located within the PBL. This fact calls into question the validity of basic assumptions behind the scheme given by Eqs. (1)–(5).

Equation (1) assumes that the evolution of the mean quantities can be computed accurately with vertical derivatives of the turbulent fluxes at the coarse mesh resolution. We can estimate the accuracy through a priori testing—a method widely used in computational fluid dynamics (e.g. Brandt 2006). The method uses exact fluxes or exact profiles of wind speed and temperature as a first-step procedure to analyse the model errors. Firstly we consider errors due to the finite-difference scheme applied to strongly curved flux profiles within the PBL. Analysis of turbulence data and large-eddy simulation modelling (Zilitinkevich and Esau 2005) suggests universal analytical dependencies for momentum and heat for a shear-driven PBL. These are:

$$\frac{F_\psi}{F_{\psi s}} = \exp\left(c_\psi (z/H)^2\right) \quad (6)$$

where $c_\psi$is a non-dimensional constant, which is –8/3 for momentum and –2 for heat fluxes, $F_{\psi s}$ is the surface flux, and H is the boundary layer height. Equation (6) can be differentiated both analytically and numerically, and the ratio between the two values gives an estimate of the error in the term $\partial\psi/\partial t$ due to the implementation of the numerical scheme at a given resolution. Figure 1 shows the tendencies, $H\,(F_{\mathrm{Ts}})^{-1}\,\partial T/\partial t = -\,(F_{\mathrm{Ts}})^{-1}\partial F_T/\partial z = -2c_T H^{-2} z\, F_T/F_{\mathrm{Ts}}$, for different meshes for a case when the heat flux is accurately known. When the heat flux is approximated with the 31L resolution, the differentiation errors lead to additional heating at the surface as well as too weak temperature changes in the PBL interior. The differentiation of the coarsely approximated fluxes may thus result in a warm surface bias in the model. The bias is clearly reduced with the refinement of the vertical resolution as shown by the results from the 90L configuration.

A more comprehensive test is based on accurate wind speed and temperature profiles from a high-resolution

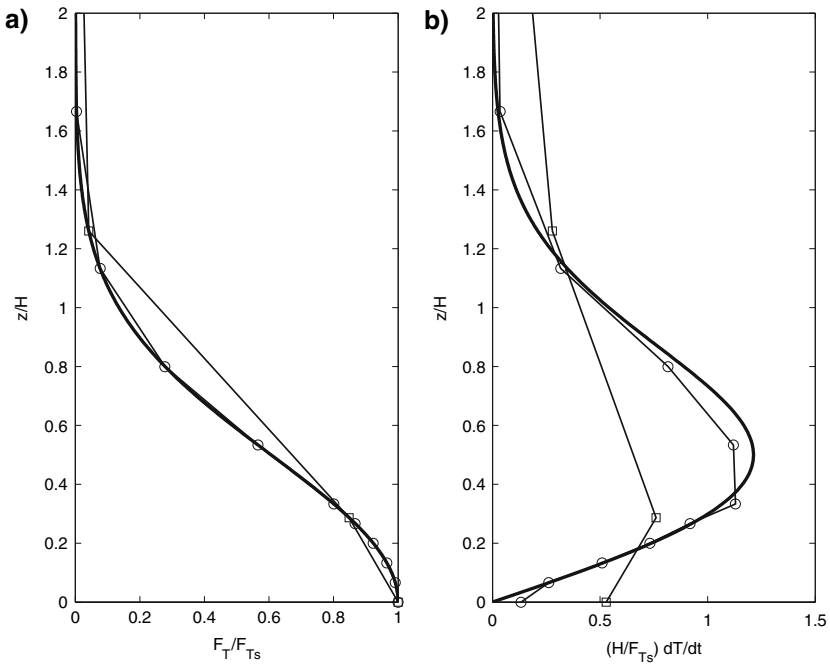

Fig. 1 **a** The exact normalized vertical temperature flux profile approximated with coarse and fine meshes. *Solid curve*, the exact universal profile in Eq. (6) derived from the turbulence-resolving simulations; *squares* connected by *thin lines*, the 31L run approximation of the profile; *circles* connected by *thin lines*, 90L run approximation of the profile. **b** The normalized temperature change induced by second-order differentiation of the exact normalized vertical temperature flux profile from **a**

turbulence—resolving model—LESNIC (Esau 2004). LESNIC employs periodic lateral boundary conditions with turbulent flux of potential temperature at the surface. The LES runs were initiated from perturbed laminar flow. We include here the LES runs that are typical for Arctic conditions. Figure 2 shows profiles for 31L, 90L approximations and LESNIC using a 128^3 mesh with a uniform vertical resolution of 4.7 m. Despite of the quite reasonably approximated wind and temperature profiles for both 31L and 90L, the gradient Richardson numbers computed from the approximations differ considerably from the LESNIC. This difference results in large errors in H for the 31L run. H is found to be 248 m using LESNIC, while it is 500 and 250 m in the 31L and 90L runs, respectively.

Figure 3 shows the normalized heat fluxes and the temperature tendencies for the turbulence schemes for 31L and 90L, LESNIC and the analytical curve described by Eq. (6). The LESNIC run presented here indicates that the imposed strong stability, a typical feature of the high-latitude atmosphere, can induce downward heat fluxes at the PBL top that are as strong as the radiative cooling at the surface. The analytical curve (Eq. 6) represents the best fit of the mean LES data for the entire range of the governing parameters. For the case presented here the turbulence-resolving model agrees with the universal curve (Eq. 6) only within the lower part of the PBL. One should expect that the turbulence schemes would be closer to the universal curve than to the full—physics turbulence—resolving simulations. Obviously this is not the case. The heat flux in the 31L approximation is about 3 times larger than in the LESNIC and mixes over a much thicker layer. The surface flux computed from the LESNIC surface temperature is inconsistent with the flux in the PBL interior. To achieve consistency between the fluxes, the surface temperature needs to be increased. Based on this inconsistency we would expect to find a warm surface bias in the ARPEGE climatology. It is thus not surprising that the ARCMIP intercomparison experiment (Tjernstrom et al. 2005) indicated no correlation between the observed and modelled surface turbulent fluxes. The unrealistically thick PBL should also exhibit less temperature variability, as it mixes a larger volume of air. This is in line with the weak model variability found in Beesley et al. (2000) in their comparison with in situ data from SHEBA. The representation of the heat flux in the 90L approximation is substantially improved in the lowest part of the PBL where the resolution is the finest. The errors in the flux and temperature tendencies increase considerably in the upper part of the PBL where the resolution deteriorates. However, at the PBL top, the stability is equally important for the correct description of the vertical turbulent mixing (see considerations of the imposed stability parameter in Zilitinkevich and Esau 2003, 2005), but neither the imposed stability parameter accounted for in the existing turbulence schemes nor the model resolution has been refined sufficiently to minimize this physical drawback of the schemes. But as seen from Fig. 2b, the stability increases in the capping inversion. The turbulence at the PBL top is relatively weak, so the overall error is smaller near the PBL top

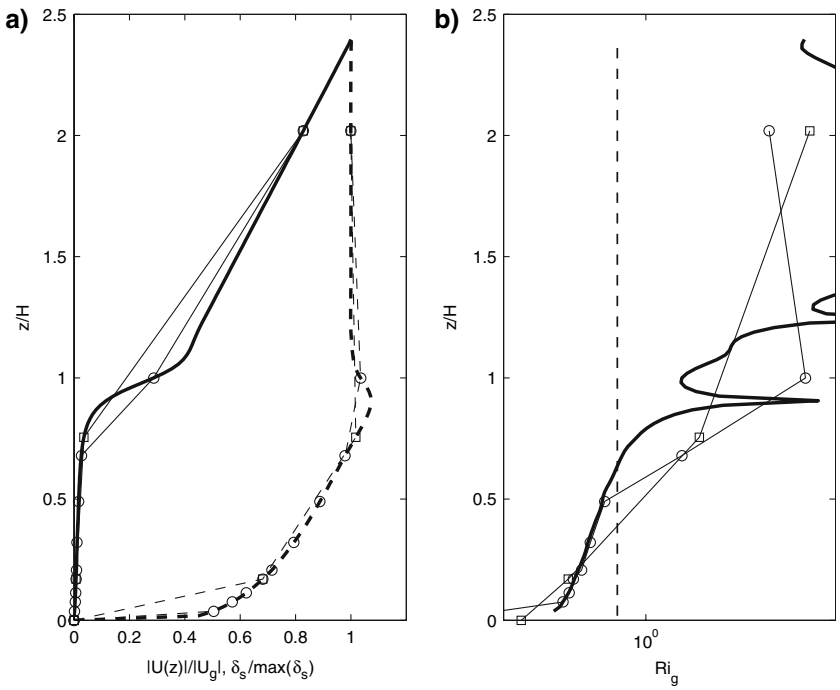

Fig. 2 **a** Approximation of exact temperature (*solid curve*) and wind (*dashed curve*) profiles taken from a 128 level run of the turbulence-resolving model LESNIC. On the horizontal axis $\delta_s = \theta(z) - \theta_s$; **b** gradient Richardson number computed from exact and approximated profiles. The *solid curves* are for the LESNIC, the PBL depth, $H = 248$ m; *squares*, the 31L approximation of the profiles; *circles*, 90L approximation. The *dashed vertical line* represents the critical Richardson number $\mathrm{Ri}_C = 0.5$

than near the surface. The surface and PBL fluxes are almost consistent in the 90L approximation, suggesting that 10 m vertical resolution seems to be adequate for the most typical Arctic PBLs. However, the inconsistency in the upper PBL will still involve excessive downward heat transport from the free (potentially warmer) atmosphere providing a small warm bias in the 90L experiment. Note as well that diffusion schemes commonly show exaggerated fluxes combined with a too-deep PBL (Cuxart et al. 2006). Cuxart et al. (2006) also indicate that even if the resolution is as fine as 6 m, the current turbulence schemes still make the largest errors at the PBL top.

4 Climatology

4.1 Description of the ERA-40 reanalysis data

In this study we have chosen to use the ERA-40 (Uppala et al. 2005) reanalysis data as a basis for the model validations and comparison. In many respects ERA-40 constitutes an improvement compared to earlier reanalysis products. The data we use are for the period January 1979–December 1997. The reliability of the ERA-40 reanalysis data is the highest after 1979 due to improvements in the observational systems (Onogi 2000). The ERA-40 reanalysis model is run with a total of 60 vertical levels of which approximately 12 are below the 850 hPa height.

Both the ARPEGE/IFS and the ECMWF (ERA-40) models define the PBL depth, H, following Troen and Mahrt (1986) (Sect. 2.1). This definition has been proved to be reasonable for the PBL developing against the free atmospheric temperature inversion as is the case in the Arctic. Intercomparison between lidar inspace technology experiment (LITE) measurements and ECMWF model results (Randall et al. 1998) suggests that the ERA-40 data overestimate the PBL depth over oceans but give reasonable agreement with the depth over land. The scatter is large however, since the diagnostic scheme in the model does not account for a number of advection and evolution effects. On basis of this intercomparison, one can expect that the typical PBL depth in the Arctic could be slightly overestimated in ERA-40. Fig. 4 shows the median wintertime (DJF) PBL depth, H, from the ERA-40 reanalysis. The median value of H reaches the smallest values over the cold Arctic land areas. The median depth of the PBL over the Arctic Ocean is typically less than 150 m. The 200 m constraint on H, as included for the 31L simulation is thus inappropriate for the Arctic PBL.

During the dark Arctic winter months, the surface temperature is highly sensitive to changes in the long-wave radiation. Clouds are important in this connection. The cloud radiative forcing is positive through the Arctic winter. The cloud fields in the ERA-40 reanalysis are shown to have considerable biases compared to observations (Bromwich et al. 2002). However a lack of basin - wide observations of clouds over the Arctic Ocean adds

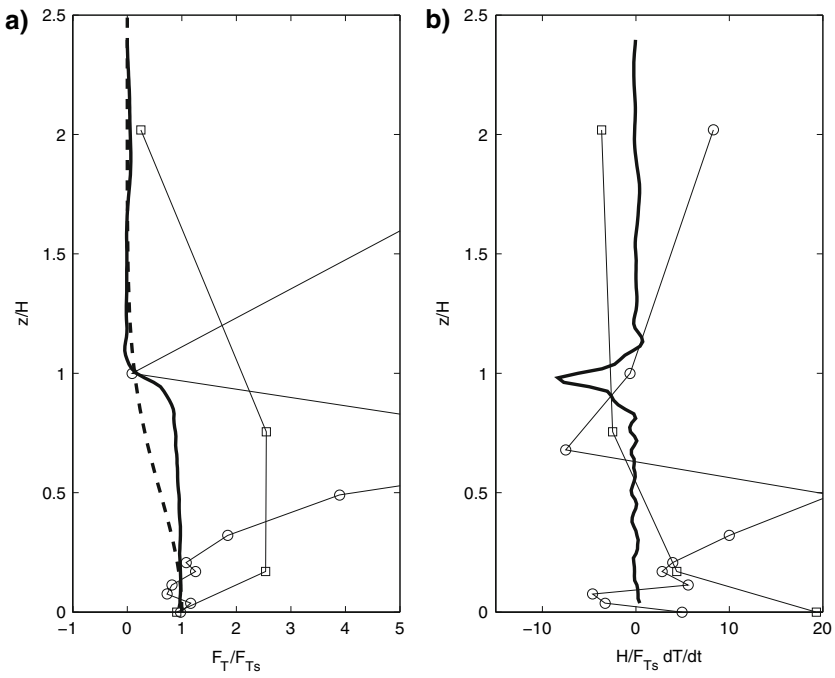

Fig. 3 Computed normalized temperature fluxes (**a**) and normalized temperature tendencies (**b**). The *solid curves* are for the data from the turbulence-resolving model LESNIC where the PBL depth, H, was 248 m; *squares*, the 31L approximation; *circles*, 90L approximation. The computation of the surface temperature was parameterized in the LESNIC since the model uses the surface fluxes as boundary conditions. Hence application of the ARPEGE bulk approximation in the surface layer result in similar surface heat fluxes in all three models. Eq. (6) is plotted as a *dashed curve* in **a**

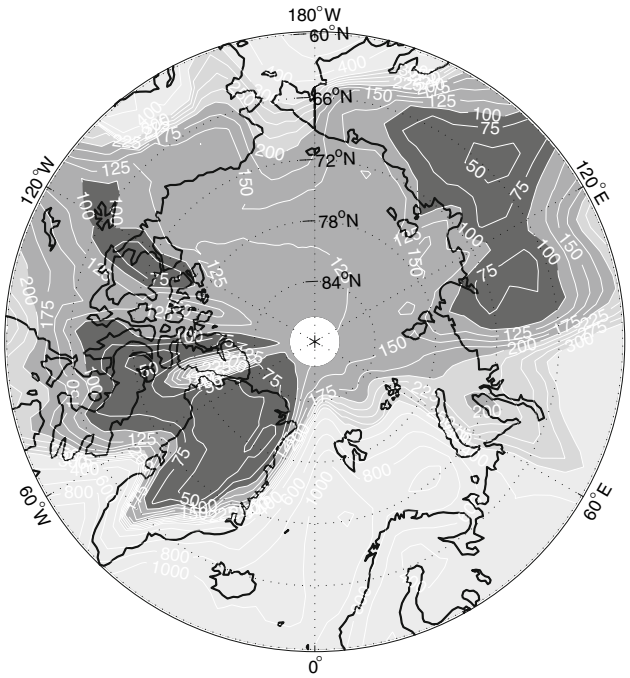

Fig. 4 Median PBL height for ERA-40 for December–February in the period 1979–1997. Contours are drawn every 25 m for values in the range 0–300 m. For values larger than 400 m the contour spacing is 200 m

uncertainty to the measured cloud fields as well (e.g., Key et al. 2004). Morcrette (2002) has found the surface clear-sky fluxes in the ERA-40 to be reasonable in comparison with surface measurements. In this paper we focus on the clear sky fluxes rather than the actual fluxes due the biases in the ERA-40 cloud fields.

The severe cold bias in the ERA-15 surface and near-surface temperatures during winter and spring over northern Eurasia and America has been corrected in ERA-40. In some areas a smaller warm bias has, however, been noted in the ERA-40 analyses, especially during springtime (e.g., Hagemann et al. 2005). A concern in the ERA-40 reanalysis is a cold bias in the lower troposphere (below about 500 hPa) over the ice-covered Arctic Ocean. A cold bias in the lower troposphere in addition to a smaller warm bias at the surface represents, on average, too-weak temperature inversions and too-low static stability in the ERA-40 reanalysis. This was confirmed by Liu and Key (2003), who found that the temperature inversions in the reanalysis data were too weak compared to the moderate resolution imaging spectrometer (MODIS) satellite data. This problem can largely be related to the low vertical resolution in the model. It would also be desirable for the ECMWF model to increase its resolution in the lower troposphere, in order to better describe the vertical exchange processes as discussed in Sect. 3. Nevertheless, compared to other alternatives, ERA-40 constitutes the best dataset with which to validate our model results.

4.2 Model climatology

Figure 5 shows the median PBL height in the model experiments, without applying the constraint of $H \geq 200$ m. The PBL in the 31L simulation is considerably

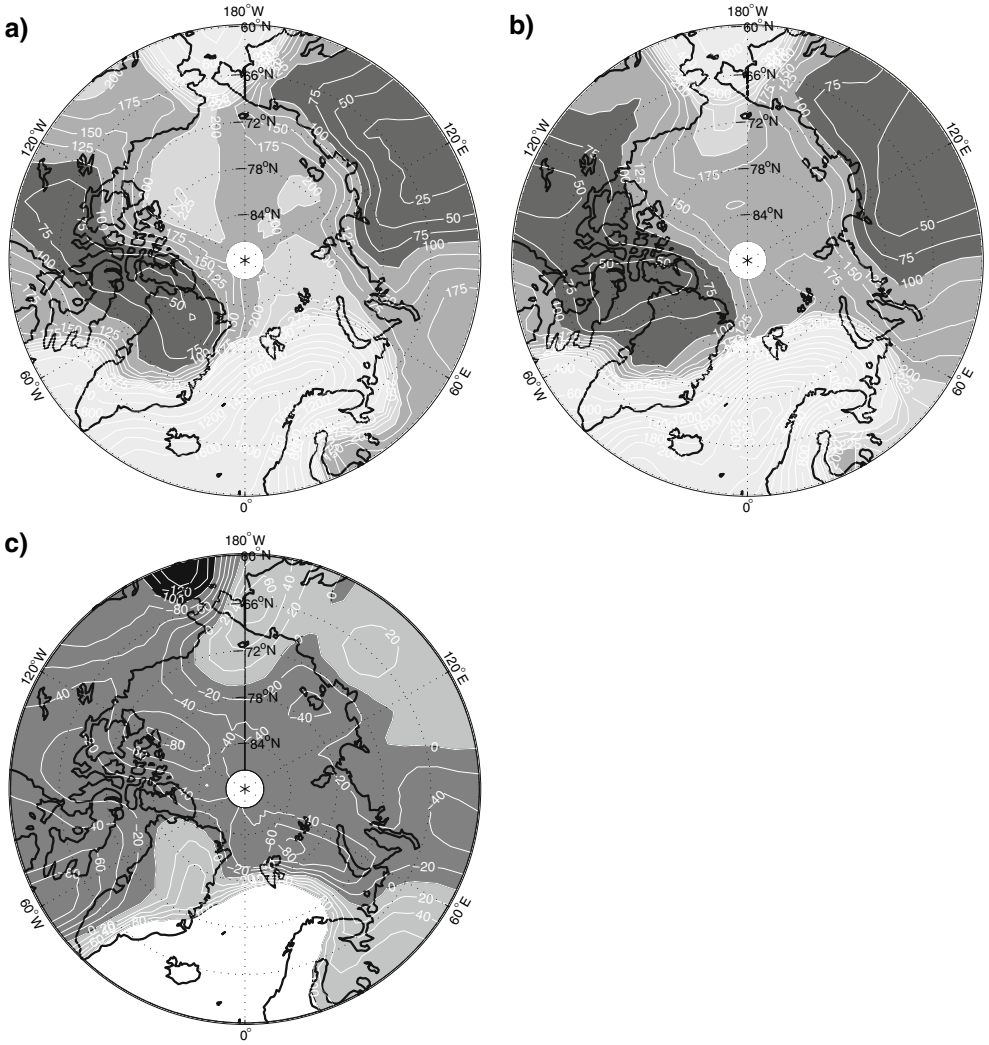

Fig. 5 Median PBL height for 31L (**a**), 90L (**b**). Contours are drawn every 25 m for values in the range 0–300 m. For values larger than 400 m the contour spacing is 200 m. **c** Shows the difference in median PBL height (90L-31L). The contour interval is 20 m

deeper than in the ERA-40 reanalysis over the Arctic Ocean with a median depth north of 80°N of 177 m. The 90L run is in this respect a clear improvement: the median PBL height is reduced to 141 m compared to 136 m for the ERA-40 climatology.

The 90L run shows an increase in static stability. The turbulent mixing is in this case restricted to a considerably shallower layer, which allows formation of radiation inversions at lower levels. This is a desired modification as indicated by Cuxart et al. (2006). The average temperature difference through the inversion layer increases from 4 K to 6 K when the vertical resolution is increased in the model. The improved representation is demonstrated in Fig. 6. This shows the average wintertime (DJF) vertical temperature profile north of 80°N. Clearly a tropospheric cold bias of –1.5 K is evident in the simulations. This can be attributed to differences in the large-scale circulation patterns in the model and/or problems related to the radiation parameterization schemes that are beyond the scope of this paper. The average SAT north of 80°N is similar in 31L and in the reanalysis; a shift toward lower SAT is evident for 90L. However, Fig. 6 represents a spatial average which incorporates areas of compensating positive and negative biases for the SAT. The important feature that relates to the vertical exchange processes is the shape of the profile. The improvement in the 90L simulation compared to 31L is evident in this respect.

The surface temperature bias over the Arctic Ocean is reduced in accordance with the reduced PBL heat fluxes in 90L (Fig. 7). The overall negative biases over high latitude land areas are most likely connected to differences in the lateral energy transports and large-scale circulation

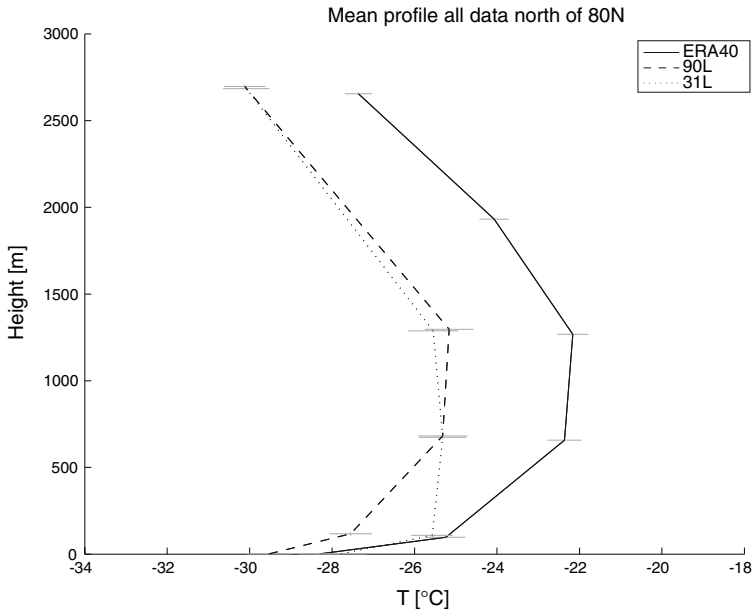

Fig. 6 Average DJF temperature (°C) profile north of 80°N for ERA-40 (*solid curve*), 31L (*dotted curve*) and 90L (*dashed curve*). The *horizontal lines* denote the 95% confidence interval for the mean value at each level

between the model and reanalysis (e.g. Walsh et al. 2002). For instance the positive trend in the NAO seen in the observations in the 1980s and 1990s (e.g. Hurrell 1995) is not reproduced in the model simulations.

Table 1 presents the mean sensible heat flux and net clear-sky radiative flux at the surface for the model simulations and for the ERA-40 reanalysis. The 31L simulation underestimates the turbulent energy transfer from the atmosphere to the surface compared to the ERA-40 data, while the sensible heat fluxes in 90L become too large in the 60°–80°N latitude bands. However, large areas of high baroclinicity are found along the ice edge at these latitudes. In these areas, larger-scale dynamic-exchange processes take place as well, which will not be discussed here. The model simulations show in general larger radiative heat loss than the reanalysis. The 90L simulation shows a considerable improvement compared to 31L in representing the net clear sky radiative balance north of 60°N as shown in Table 1.

In the cold wintertime Arctic atmosphere, the maximum long-wave radiation is shifted to the so-called "dirty" window between 18 and 25 μm, where specific humidity determines opacity of the atmosphere. Thus, the radiative cooling rate becomes sensitive to the accuracy of the temperature and humidity simulated in the lower troposphere. Moreover, the relative humidity and thereby cloudiness are sensitive to the inversion temperature as the low-level clouds tend to form within the inversion layer.

We generally see a reduction of moisture in the PBL when the vertical resolution is increased, this also affects low-level cloudiness in the model. This feature is in agreement with the effect of reduced vertical turbulent mixing. The cloud cover north of 80°N for the two simulations and for the reanalysis is presented in Table 2 for low and total cloud cover amounts during the winter months. For comparison, estimated total cloud cover from surface based observations (Arctic Climatology Project 2000) and satellite measurements from the international satellite cloud climatology project (ISCCP) (Rossow and Schiffer 1999) and TIROS operational vertical sounder (TOVS) (Francis and Schweiger 1999) are shown. In the 90L simulation, the average total cloud cover is reduced by 10% compared to 31L. The Arctic cloud cover is systematically shifted to lower values for all months of the year. A large reduction is found for the low-cloud-cover field, consistent with the reduction of relative humidity in the boundary layer. Both model simulations produce less cloud cover than the ERA-40 over the Arctic Ocean. The reanalysis however reports more clouds than suggested by the observational estimates.

The problems related to the biases in cloud cover in the Arctic are complicated by the different parameterizations used for clouds, radiation and for turbulence diffusion. Moreover, to keep the models on track, a number of tuning parameters have been introduced. The parameters from the different schemes interact. A comprehensive re-tuning would thus be required to gain an improved physical representation for all these parameterization schemes.

The response in the cloud cover fields illustrates a substantial sensitivity in the cloud schemes to the vertical resolution. Such a high sensitivity to the vertical resolution has also been found by Lane et al. (2000) using a single column model.

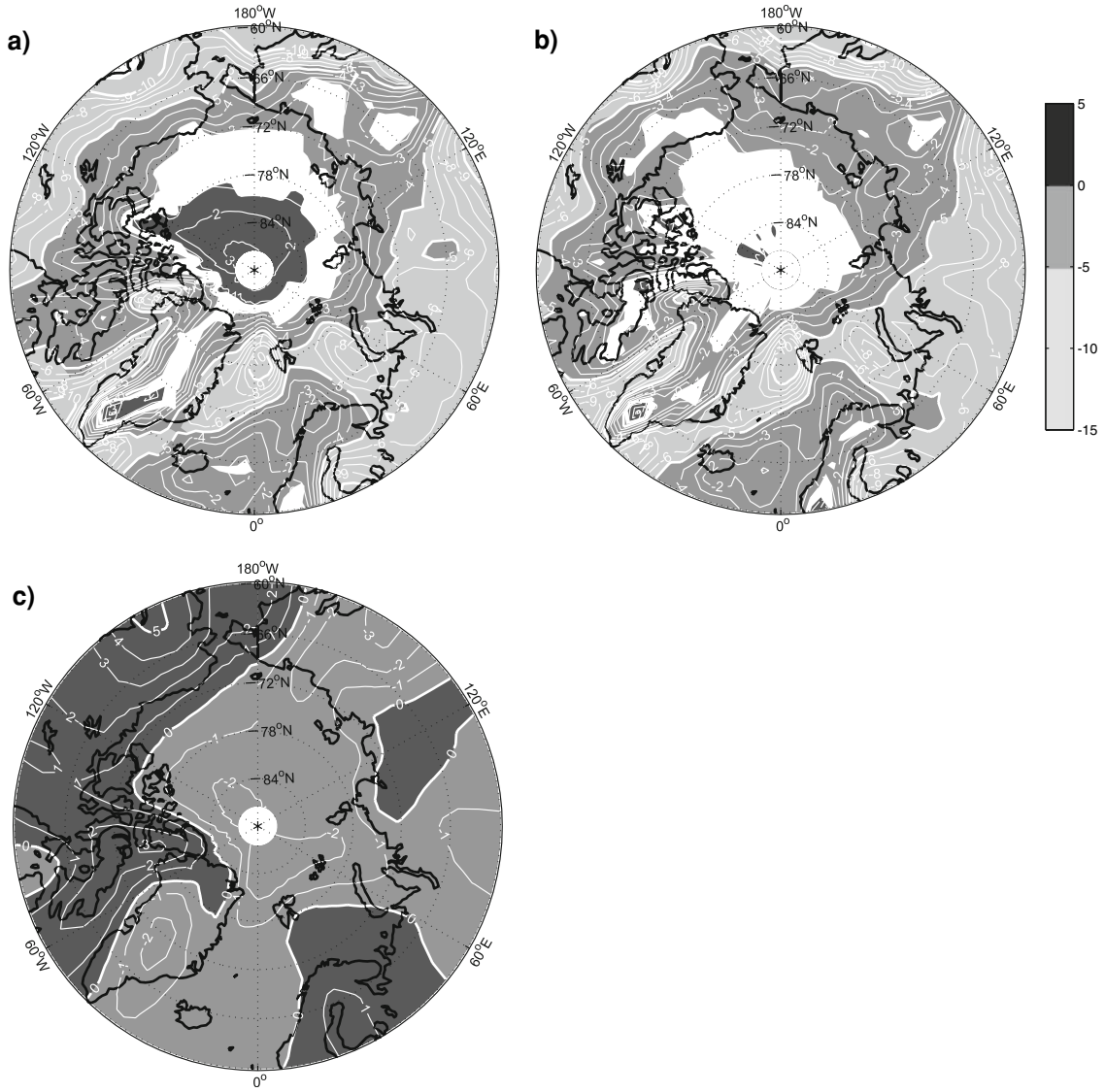

Fig. 7 Bias in surface air temperature (K) in 31L (**a**) and 90L (**b**) compared to ERA-40. The biases shown are significantly different from zero at the 5% level. The difference 90L – 31L is shown in **c**. Contours are drawn every 1 K. The data are for December–February in the period 1979–1997

Table 1 Averages of sensible heat flux (SH) and net clear sky radiative heat flux (net R) at the surface for ERA-40, 31L and 90L for different latitude bands

	Latitudes (°N)	ERA40 (W m^{-2})	31L (Wm^{-2})	90L (Wm^{-2})
SH	80–90	11.2	6.0	10.6
	70–90	5.3	2.1	7.6
	60–90	5.8	1.2	7.4
Net R	80–90	–64.2	–74.9	–69.0
	70–90	–67.3	–74.5	–69.8
	60–90	–66.6	–71.5	–67.6

The data are averages for December–February in the period 1979–1997

5 Physical characteristics

Zilitinkevich and Esau (2003) provided a quite robust analytical dependence between the PBL depth and the external governing parameters like the friction velocity, surface sensible-heat flux and the free-atmosphere stratification. Furthermore, Zilitinkevich and Esau (2005) developed analytical formulations for the resistance laws. The above works demonstrated that properties of the Arctic PBL are different in weak-wind and strong-wind regimes, as well as for weak and strong atmospheric inversions.

The relation between surface winds and surface air temperature for the model simulations and ERA-40 is demonstrated in Fig. 8. The slope of the curve in Fig. 8d

denotes the relation between SAT and surface wind speed. Typically, light surface winds correlate to low SAT, while stronger winds are related to enhanced vertical mixing and thus larger turbulent heat fluxes and higher SAT. The stronger winds tend to mix warmer air from higher up in the inversion down to the surface. The two model runs and the reanalysis data follow different characteristics. In the light wind regime (0–6 m/s) there is a considerable scatter between the simulations and the reanalysis. The reanalysis data for light winds are generally associated with lower SAT than what is the case for the model simulations. The 90L simulation is in this regard more similar to ERA-40 than the 31L simulation.

Table 2 Total and low wintertime cloud cover averaged over the Arctic Ocean for ERA-40, 31L and 90L

	ERA40	31L	90L	EWG	ISCCP-D2	TOVS
Total cloud cover	79.4	69.8	59.0	56.3	71.8	69.6
Low cloud cover	66.0	58.8	52.7	16.5	5.5	–

Data from surface based observations (EWG) and satellite-based observations (ISCCP-D2 and TOVS) are also presented. The units are in percentage

The overall SAT sensitivity to changes in the wind speed is generally higher for the reanalysis data than for the model simulations. For winds stronger than 3 m/s, the ERA-40 SAT is clearly related to wind speed. For light winds below 3 m/s ERA-40, SAT shows small or no

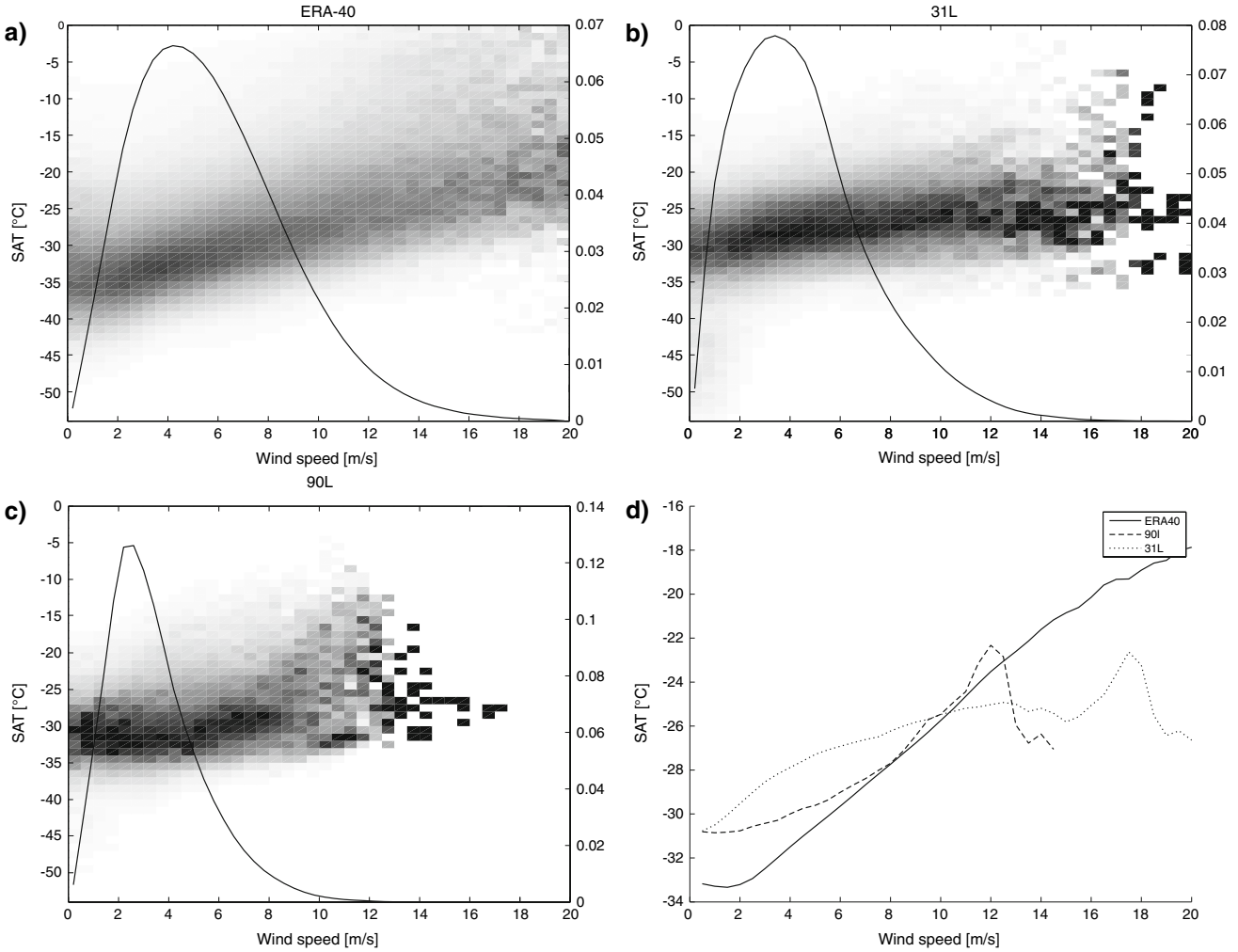

Fig. 8 Relation between surface winds (10 m) and surface (2 m) air temperature. **a**–**c** Show the density of surface temperature divided in bins of surface winds (*grey scatter*). This represents the spread around the mean for each value of surface wind. *Dark shading* represents high density. The *black curve* represents the distribution of wind speed. The distribution is for **a** ERA-40, **b** 31L, and **c** 90L. SAT (°C) is on the left vertical axis, surface wind speed (m/s) on the horizontal axis, *p* value for wind speed distribution on the right vertical axis. **d** Shows the relation between wind and average SAT for ERA-40, 31L and 90L. The data are for December–February in the period 1979–1997

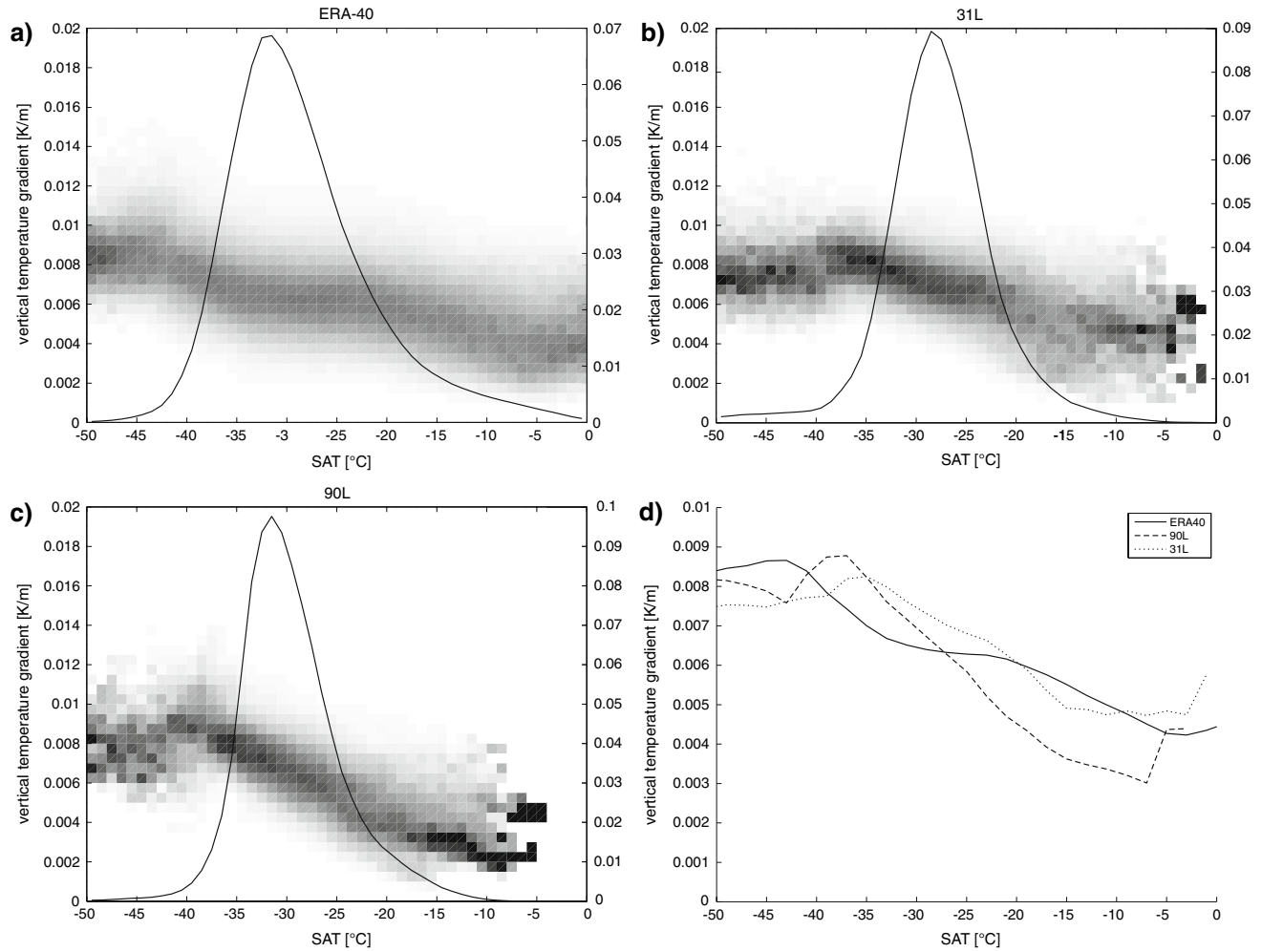

Fig. 9 Relation between surface (2 m) air temperature and vertical temperature gradient in the 700–850 hPa layer. **a–c** Show the density of $\partial\theta/\partial z$ divided in bins of SAT (*grey scatter*). This represents the spread around the mean for each value of SAT. *Dark shading* represents high density. The *black curve* represents the distribution of SAT. The distribution is for **a** ERA-40, **b** 31L, and **c** 90L. $\partial\theta/\partial z$ (K/m) is on the left vertical axis, SAT (°C) on the horizontal axis, p value for the SAT distribution on the right vertical axis. **d** Shows the relation between SAT and average $\partial\theta/\partial z$ for ERA-40, 31L and 90L. The data are for December–February in the period 1979–1997

sensitivity to the surface winds. The light winds (less than 3 m/s) are associated with only weak turbulence, which might be too weak to penetrate the capping inversion to bring warmer air down to the surface.

The 90L simulation maintains a low sensitivity for light winds. The sensitivity gradually increases with increasing wind speed. For winds stronger than 5 m/s, 90L shows a relation between SAT and wind speed which is similar to the reanalysis.

The relation between wind speed and SAT is somewhat different for the 31L simulation. The 31L simulation shows a strong relation between SAT and wind speed in the lower part of the range (below 3 m/s). This relation is less clear for winds stronger than 6 m/s. This illustrates that for 31L, even winds in the lower range seems to easily penetrate the capping inversion and mix warmer air down to the surface. This is in line with the notion of too-large vertical mixing in the lower troposphere in 31L. For winds in the range 0–6 m/s, the average temperature simulated for 31L are systematically 3–4°C higher than for ERA-40.

For wind speeds above 12 m/s, ERA-40 shows generally the same relation between surface winds and SAT as for more moderate wind speeds. The 90L and 31L simulations generally predict weaker surface winds than ERA-40, and show considerable scatter in this part of the range. Strong surface winds are related to deeper boundary layers (Eq. 4). For deeper boundary layers, we expect to see less improvement in the simulations because the PBL in general will be resolved by several model levels also in 31L.

Figure 9 shows the relation between the vertical gradient in potential temperature in the 850–700 hPa layer $(\delta\theta/\delta z = (\theta_{700} - \theta_{850})/(z_{700} - z_{850}))$ and SAT. In the simulations and ERA-40 data, SAT generally decreases

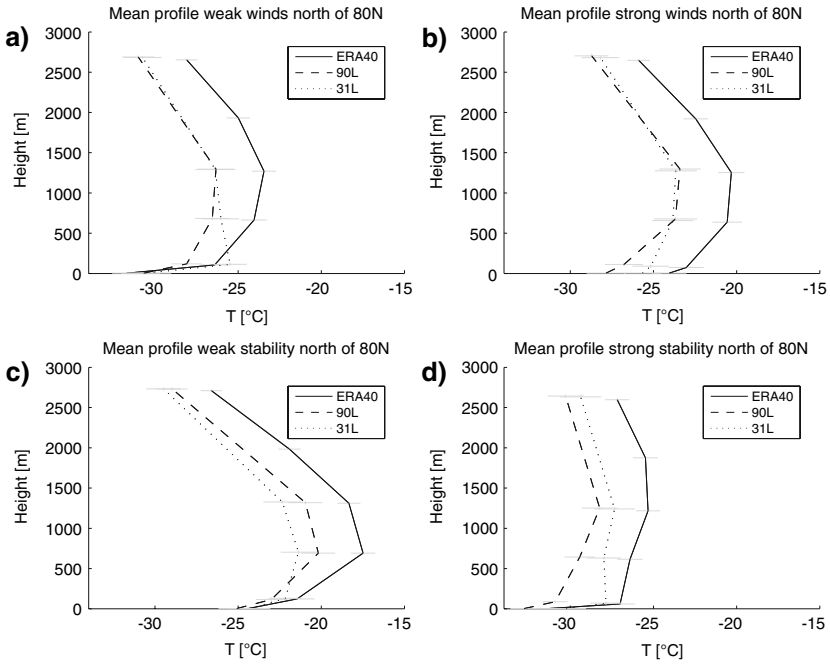

Fig. 10 Same as Fig. 6, but for 4 different cases separated by upper and lower quartiles of key governing parameters. The separation is based on surface wind speed and average vertical gradient in potential temperature in the 700–850 hPa layer ($\partial\theta/\partial z$). The average temperature profiles are plotted for the cases with **a** the 25% weakest surface winds, **b** the 25% strongest surface winds, **c** the 25% weakest temperature gradients and **d** the 25% strongest temperature gradients

with increasing stratification in the free atmosphere. Simulated SATs, in particular 90L, are more strongly correlated to $\delta\theta/\delta z$ than are the reanalysis data. Both simulations show a strong relation for SAT in the range –40°C to –15°C. The majority of simulated data falls within this range, illustrating that the free atmosphere stability relates quite strongly to the simulated SAT.

In comparison with ERA-40 the physical mechanisms that govern the vertical exchange processes in stable PBLs, are represented more accurately in 90L than in the 31L simulation. This is demonstrated in Fig. 6. Figure 10 shows the dependence of the temperature on key governing parameters in a panel plot for 4 regimes. The regimes are determined as quartiles in the overall wind and stability distribution functions north of 80°N in 90L, 31L and ERA-40. The 90L simulation shows an overall improvement for all the four regimes in comparison with 31L.

6 Discussion

Surface wind speeds are generally too low in the model (31L), the average wind speed being 4.6 m/s in the area north of 70°N, compared to ERA-40 data which have an average wind speed of 5.9 m/s. The biases in the surface winds are related to even larger biases in the momentum fields above the boundary layer at 850 and 700 hPa levels. The biases in the wind fields in the control simulation (31L) might be related to biases in the general large-scale circulation patterns in the model and will not be discussed in more detail here.

The surface winds in 90L are reduced in comparison to 31L. This may be related to the stronger stratification in the boundary layer in this simulation. The entrainment of momentum from the free atmosphere down to the surface is reduced. The negative bias in the surface wind speeds increases from 1.3 m/s in 31L to 2.2 m/s in 90L. The biases at 850 hPa level are –2.4 m/s for 31L and –2.9 m/s for 90L. This is in accordance with the Prandtl relation employed in the model parameterisation: a reduction in the vertical momentum flux will follow the reduction in the vertical heat flux. Cuxart et al. (2006) evaluated several parameterizations of the stable boundary-layer exchange processes and found that the vertical fluxes of heat and momentum were generally overestimated compared to LES data in most of the parameterizations employed in the large-scale climate models. Although the bias in the surface wind increases in 90L, the reduction of the vertical momentum flux should constitute an improved representation of stable boundary-layer exchange processes.

7 Conclusions

Surface–atmosphere exchange in the wintertime Arctic is inhibited by strong stratification in the shallow boundary layer capped by a temperature inversion. This boundary layer cannot be properly resolved by the vertical resolution in the standard version of the ARPEGE/IFS climate model. This is also the situation for the majority of the IPCC climate models. For a coarse vertical mesh (the 31L run with 31 model levels) the vertical diffusion

parameterizations are shown to be inaccurate. For the first order closure scheme the main assumption is that the vertical fluxes in stably stratified boundary layers are determined by the vertical temperature and momentum gradients. Due to the strongly curved profile in the Arctic stable boundary layer, the poor resolution leads to inaccurate fluxes and gradients. The eddy-viscosity schemes commonly applied in the GCMs are related to excessive-turbulent heat fluxes in the Arctic stable boundary layer. To study the effect of the parameterization failure, we performed simulations with a fine mesh (90L with 90 vertical levels). The vertical mesh for the high-resolution run was chosen in accordance with quality criteria based on data from large eddy simulations.

Comparison of the two simulations with ERA-40 reanalysis during wintertime in the Arctic revealed a high sensitivity to the mesh refinement. By utilizing a high vertical resolution we achieved a better simulation of physical processes in the boundary layer. The depth of the PBL simulated with 90L was in better accordance with data from ERA-40, whereas the PBL of 31L in general was too deep. The turbulent fluxes of both heat and momentum were reduced accordingly in the high resolution run.

Furthermore, the inversion and low surface temperatures were improved compared to the 31L simulation. A warm bias was evident over the Arctic Ocean in 31L. This bias was significantly reduced in 90L. Surface fluxes and the radiation balance were also improved in 90L. The SAT sensitivity to changes in surface winds increased in 90L and became more similar to the relation found from ERA-40 reanalysis data.

For the surface wind field, we found a negative bias in the 31L simulation, the reduction of the vertical momentum flux in 90L further amplified this bias. The bias in the surface wind field is related to larger differences in the momentum fields in the free atmosphere. A more comprehensive study of the sensitivity in the large-scale circulation patterns will be required to give an explanation of these biases.

In this paper we have not considered changes in the large-scale circulation patterns, although one would expect an improved representation of the stable boundary layer to be linked to an overall improvement in simulating the large-scale climate as well. However, such an improvement might be veiled by the natural variability, feedback effects in the climate system or the interaction between the different parameterization schemes.

The computational cost to run the model with such a high vertical resolution (90L) has been approximately 6 times larger than for the traditional 31L simulation. Therefore, the large increase in the computational costs at this point does not support running the model with 90L in future GCM simulations. Nevertheless, this study demonstrates the potential for improving the parameterization of the stable PBL. Whether a more moderate choice of vertical resolution in the PBL also would give beneficial effects on simulations of the stable boundary layer is a question for further research.

Acknowledgments ECMWF ERA-40 data used in this study have been obtained from the ECMWF data server. This work has been supported by the Norwegian project MACESIZ 155945/700, joint Norwegian-USA project ROLARC 151456/720, and the PAACSIZ 178908/S30. This is publication number A 177 from the Bjerknes Centre for Climate Research. The authors whish to thank Dr. Martin Miles for valuable comments on the manuscript.

References

ACIA (2004) Arctic climate impact assessment. Cambridge University Press, Cambridge, pp 140

Arctic Climatology Project (2000) Environmental working group Arctic meteorology and climate atlas. In: Fetterer F, Radionov V (eds) Boulder (CD-ROM). National Snow and Ice Data Center, Colorado

Bazile E, Beffrey G, Joly M, Marzouki H (2005) Interactive mixing length and modifications of the exchange coefficient for the stable case. Newsletter ALADIN, Météo-France/CNRM/GMAP

Beare RJ, Macvean MK, Holtslag AAM, Cuxart J, Esau I, Golaz J-C, Jimenez MA, Khairoutdinov M, Kosovic B, Lewellen D, Lund TS, Lundquist JK, Mccabe A, Moene AF, Noh Y, Raasch S, Sullivan P (2006) An intercomparison of large-eddy simulations of the stable boundary layer. Boundary-Layer Meteorol 118(2):247–272

Beesley JA, Bretherton CS, Jakob C, Andreas EL, Intrieri JM, Uttal TA (2000) A comparison of cloud and boundary layer variables in the ECMWF forecast model with observations at surface heat budget of the Arctic Ocean (SHEBA) ice camp. J Geophys Res Atmos 105(D10):12337–12349

Beljaars A, Viterbo P (1999). The role of the boundary layer in a numerical weather prediction model. In: Holtslag AAM, Duynkerke PG (eds) Clear and cloudy boundary layers. Royal Netherlands Academy of Arts and Sciences, Netherlands, pp 287–304

Bossuet C, Deque M, Cariolle D (1998) Impact of a simple parameterization of convective gravity-wave drag in a stratosphere-troposphere general circulation model and its sensitivity to vertical resolution. Ann Geophys Atmos Hydrospheres Space Sci 16(2):238–249

Boville BA (1991) Sensitivity of simulated climate to model resolution. J Clim 4(5):469–485

Brandt T (2006) A priori tests on numerical errors in large eddy simulation using finite differences and explicit filtering. Int J Numer Methods Fluids 51(6):635–657

Bromwich DH, Wang S-H, Monaghan AJ (2002) ERA-40 representation of the arctic atmospheric moisture budget. ERA-40 Rep Ser 3:287–297

Bushell AC, Martin GM (1999) The impact of vertical resolution upon GCM simulations of marine stratocumulus. Clim Dyn 15(4):293–318

Chapman WL, Walsh JE (2007) Simulations of Arctic temperature and pressure by global coupled models. J Clim 20(4):609–632

Cuxart J, Holtslag AAM, Beare RJ, Bazile E, Beljaars A, Cheng A et al (2006) Single-column model intercomparison for a stably stratified atmospheric boundary layer. Boundary Layer Meteorol 118(2):273–303

Deque M, Dreveton C, Braun A, Cariolle D (1994) The Arpege/Ifs atmosphere model—a contribution to the French community climate modeling. Clim Dyn 10(4–5):249–266

Dethloff K, Abegg C, Rinke A, Hebestadt I, Romanov VF (2001) Sensitivity of Arctic climate simulations to different boundary-layer parameterizations in a regional climate model. Tellus Ser Dyn Meteorol Oceanogr 53(1):1–26

Esau I (2004) Simulation of Ekman boundary layers by large eddy model with dynamic mixed subfilter closure. Environ Fluid Mech 4(3):273–303

Francis J, Schweiger A (1999) TOVS Pathfinder Path-P daily Arctic gridded atmospheric parameters. National Snow and Ice Data Center, Boulder

Furevik T, Bentsen M, Drange H, Kindem IKT, Kvamsto NG, Sorteberg A (2003) Description and evaluation of the bergen climate model: ARPEGE coupled with MICOM. Clim Dyn 21(1):27–51

Geleyn J-F (1988) Interpolation of wind, temperature and humidity values from model levels to the height of measurement. Tellus Ser A Dyn Meteorol Oceanogr 40A:347–351

Gleckler P (1996) AMIP II Guidelines AMIP Newsletter No. 8, Program for Climate Model Diagnosis and Intercomparison: http://www-pcmdi.llnl.gov/projects/amip/NEWS/amipnl8

Hagemann S, Arpe K, Bengtsson L (2005) Validation of the hydrological cycle of ERA-40. ERA-40 Report, Series 24

Hogan TF, Brody LR (1993) Sensitivity studies of the navy's global forecast model parameterizations and evaluation of improvements to NOGAPS. Mon Weather Rev 121:2373–2395

Hurrell JW (1995) Decadal trends in the North-Atlantic oscillation—regional temperatures and precipitation. Science 269(5224):676–679

Kalnay E, Kanamitsu M, Kistler R, Collins W, Deaven D, Gandin L et al (1996) The NCEP/NCAR 40-year reanalysis project. Bull Am Meteorol Soc 77(3):437–471

Key EL, Minnett PJ, Jones RA (2004) Cloud distributions over the coastal Arctic Ocean: surface-based and satellite observations. Atmos Res 72:57–88

Kiehl JT, Gent PR (2004) The community climate system model, version 2. J Clim 17(19):3666–3682

Lane DE, Somerville RCJ, Iacobellis SF (2000) Sensitivity of cloud and radiation parameterizations to changes in vertical resolution. J Clim 13(5):915–922

Liu YH, Key JR (2003) Detection and analysis of clear-sky, low-level atmospheric temperature inversions with MODIS. J Atmos Oceanic Technol 20(12):1727–1737

Louis JF (1979) Parametric model of vertical eddy fluxes in the atmosphere. Boundary Layer Meteorol 17(2):187–202

Mahrt L, Vickers D (2006) Extremely weak mixing in stable conditions. Boundary Layer Meteorol 119(1):19–39

Morcrette JJ (2002) The surface downward longwave radiation in the ECMWF forecast system. J Clim 15(14):1875–1892

Onogi K (2000) The long-term performance of the radiosonde observing system to be used in ERA-40. ERA-40 Rep Ser 2:77

Overland JE, Guest PS (1991) The Arctic snow and air-temperature budget over sea ice during winter. J Geophys Res Oceans 96(C3):4651–4662

Randall D, Shao Q, Branson M (1998) Representation of clear and coudy boundary layers in climate models. In: Holtslag AAM, Duynkerke PG (eds) Clear and coudy boundary layers. North Holland Publishers, Amsterdam, pp 305–322

Roeckner E, Brokopf R, Esch M, Giorgetta M, Hagemann S, Kornblueh L et al (2006) Sensitivity of simulated climate to horizontal and vertical resolution in the ECHAM5 atmosphere model. J Clim 19(16):3771–3791

Rossow WB, Schiffer RA (1999) Advances in Understanding Clouds from ISCCP. Bull Am Meteorol Soc 80(11):2261–2287

Ruti PM, Di Rocco D, Gualdi S (2006) Impact of increased vertical resolution on simulation of tropical climate. Theor Appl Clim 85(1–2):61–80

Simmons AJ, Burridge DM (1981) An energy and angular-momentum conserving vertical finite-difference scheme and hybrid vertical-coordinates. Mon Weather Rev 109(4):758–766

Slingo A, Hodges KI, Robinson GJ (2004) Simulation of the diurnal cycle in a climate model and its evaluation using data from Meteosat 7. Q J R Meteorol Soc 130(599):1449–1467

Smith TM, Reynolds RW (2004) Improved extended reconstruction of SST (1854–1997). J Clim 17(12):2466–2477

Tjernstrom M, Zagar M, Svensson G, Cassano JJ, Pfeifer S, Rinke A et al (2005) Modelling the arctic boundary layer: an evaluation of six arcmip regional-scale models using data from the Sheba project. Boundary Layer Meteorol 117(2):337–381

Tompkins AM, Emanuel KA (2000) The vertical resolution sensitivity of simulated equilibrium temperature and water-vapour profiles. Q J R Meteorol Soc 126(565):1219–1238

Troen I, Mahrt L (1986) A simple-model of the atmospheric boundary-layer—sensitivity to surface evaporation. Boundary Layer Meteorol 37(1–2):129–148

Uppala SM, Kallberg PW, Simmons AJ, Andrae U, Bechtold VD, Fiorino M et al (2005) The ERA-40 re-analysis. Q J R Meteorol Soc 131(612):2961–3012

Walsh JE, Kattsov VM, Chapman WL, Govorkova V, Pavlova T (2002) Comparison of Arctic climate simulations by uncoupled and coupled global models. J Clim 15(12):1429–1446

Zilitinkevich SS, Esau IN (2003) The effect of baroclinicity on the equilibrium depth of neutral and stable planetary boundary layers. Q J R Meteorol Soc 129(595):3339–3356

Zilitinkevich SS, Esau IN (2005) Resistance and heat-transfer laws for stable and neutral planetary boundary layers: old theory advanced and re-evaluated. Q J R Meteorol Soc 131(609):1863–1892